

# Equilibrium and Nonequilibrium Quantum Correlations Between Two Accelerated Detectors

He Wang<sup>1,2</sup>, Jin Wang<sup>3\*</sup>

<sup>1</sup>College of Physics, Jilin University, Changchun 130021, China

<sup>2</sup>State Key Laboratory of Electroanalytical Chemistry, Changchun Institute of Applied Chemistry, Changchun 130021, China

<sup>3</sup>Department of Chemistry and of Physics & Astronomy, Stony Brook University, Stony Brook, NY 11794-3400, USA

\*: Correspondence should be addressed to Jin Wang; [jin.wang.1@stonybrook.edu](mailto:jin.wang.1@stonybrook.edu)

## Abstract

Despite the efforts, it is still challenging to quantify the quantum correlations in the curved space time. It has long been realized that the effect of the local acceleration or the related space-time curvature is equivalent to a thermal temperature bath termed as Unruh effect. The two accelerated observers can detect quantum correlations between them through the vacuum field. A natural question arises: Can we quantify the quantum correlations between the two accelerated detectors or equivalently between two locations in curved space time and are these equilibrium (equal accelerations of the two detectors) quantum correlation equivalent to the ones between the two stationary detectors under a thermal bath? A further question is what if the two accelerations or the couplings between the detectors and vacuum field are different and how this nonequilibrium effect can influence the quantum correlations. In this study, we examine the above scenarios. We found that as the acceleration of the detectors increase, the quantum correlations (entanglement, mutual information, discord) will increase first and eventually decay depending on the redshift effect. The temperature and acceleration characterizing the equivalent space-time curvature show different impacts on the global quantum correlations in this equilibrium (equal temperatures or accelerations of the two detectors) scenario. When the equal acceleration is in the opposite direction, as the distance increases, the correlation will decay, and the entanglement appears to be more robust than the quantum mutual information and discord. Importantly, we have uncovered that the nonequilibriumness characterized by the degree of the detailed balance breaking due to the different couplings of the detectors to the vacuum field can increase the quantum correlations. We also uncovered both the nonequilibrium (different accelerations of the two detectors or equivalently different space time curvatures) and distance effects on quantum correlations between the detectors.

## I. Introduction

Quantum information has remarkable progress in the last three decades [1] and promises even more revolutionary advances in the next decades. Quantum information is often characterized by certain quantum correlation measures such as entanglement, mutual information, discord etc. Entanglement has been thought to be responsible for the spooky action over distance with quantum non-locality [2]. It is a key resource in quantum computation and information which has been studied intensively [3]. It was shown that entanglement has the pure quantum natures leading to an advantage over classical computation. Quantum mutual information is a generalization of the classical mutual information characterizing the quantum correlations between the two systems [4]. The quantum discord is the non-classical part of the correlations characterized by the difference between the quantum mutual information and classical correlation [5].

It is worth noticing that most of the studies on quantum information and quantum correlation studies concentrate on the cases when the space-time is flat. In early universe, cosmology and astrophysics, the curved space-time is unavoidable and needs to be seriously considered. [6-12]. However, the quantification of quantum correlations in the curved space time is still challenging. Furthermore, how the quantum correlations are influenced by the environment is also not so clear in curved space time. To understand the quantum information and correlations in curved space time, we can start with a simple example, the accelerated detectors. It has long been realized that the effect of the local acceleration or the related curved space-time is equivalent to a thermal temperature bath, termed as Unruh effect or Hawking effect [13,14]. Therefore, a natural question arises: Can we quantify the quantum correlations between two accelerated detectors or equivalently between two locations in curved space time? Are the equilibrium (same accelerations of the two detectors) quantum correlations between the two accelerated detectors or two locations of the curved space-time equivalent to the two stationary detectors under thermal temperature bath in flat space- times? Moreover, what if the two accelerations (or the related curvatures of the space-times) or the couplings between the detectors and vacuum field are different and how this nonequilibrium effect can influence the quantum correlations.

Quantum field theory (QFT) born from the marriage of special relativity and quantum mechanics [15] is suitable for studying the relativistic quantum information process. Some studies explored the entanglement between the field modes. It was shown that entanglement is observer-dependent and degraded from the perspective of the observers in uniform acceleration due to the Unruh effect.[6-8] As the researchers become more interested in the entanglement or quantum correlations between the observers, particle detector models, such as the Unruh-Dewitt models, were used to show the entanglement harvesting from the coupling of the detectors to a vacuum state of a quantum field [11,12,16-19]. The detector is usually made of a qubit and has been shown to be useful for investigating the quantum correlations between the detectors.[11,12,19] There have also been approaches replacing the qubit by a harmonic oscillator to serve as the detector more realistically and computing the quantum correlations

between the detectors through solving the Heisenberg equations of motion at different settings. [20,21] Furthermore, a method was developed by Eric G. Brown et al. [22] to solve the time evolution of the particle detection for the accelerated detectors with a time dependent quadratic Hamiltonian under arbitrary number of modes in a stationary cavity. The method has the advantage of gaining the time trajectories of an arbitrary number of detectors coupled to the vacuum field in the cavity without the need of the usual Bogoliubov transformation. By replacing a qubit (two energy levels) with an harmonic oscillator (infinite energy levels) in the detector model, one gains significant advantages over the standard Unruh-DeWitt (qubit-based) detector including the practical particle detection and non-perturbative treatment [22]. Therefore, the quantum evolution of particle detection can be solved nonperturbatively by using the symplectic formalism for Gaussian states and operations. [22] The evolution of particle detection can then be obtained by solving (in general numerically) a set of coupled first-order ordinary differential equations. This formalism is especially useful for scenarios of interest in relativistic quantum theory involving quadratic Hamiltonians. However, both the quantum correlations of the two equally accelerated observers for the comparison to the corresponding stationary detectors under the common thermal temperature bath and the quantum correlations of the two different accelerated observers for the comparison to the corresponding stationary detectors under two different thermal temperature baths are still not fully explored.

In this study, we consider two accelerated detectors moving inside a stationary cavity in flat space time. We found that the quantum correlations between the two accelerated detectors or the related curved space times are different from the quantum correlation between the two stationary detectors in a thermal field with the temperature  $T$ . The detectors themselves are often considered effectively surround by two thermal bathes associated with Unruh temperature  $T = \frac{a}{2\pi}$  where  $a$  is the proper acceleration of the detector.[13] As the temperature of the stationary detectors increase, the entanglement gradually disappears, while the mutual information and the quantum discord are amplified as suggested before [23]. This shows that the quantum mutual information and discord are more robust on the environmental (field) temperature fluctuations than the entanglement. However, for the accelerated detector case, as the acceleration of the detectors increases, the entanglement, mutual information and quantum discord will increase first and eventually decay. We suggest that is partly resulted from the redshift effect. The temperature and local acceleration or space-time curvature show different impacts on the global quantum correlations. When the accelerations of the detectors are in the opposite direction, the distance increases, and the quantum correlation decays. Remarkably, the entanglement seems to be more robust than the quantum mutual information and quantum discord.

In the meanwhile, we study the nonequilibrium effect on the quantum correlations where the nonequilibriumness is characterized by the degree of the detailed balance breaking due to the different couplings of the two equally accelerated detectors to the vacuum field. We show that the nonequilibriumness can increase the quantum correlations. Another nonequilibrium scenario we consider is when the two detectors are under different accelerations or equivalently different space time curvatures mimicking the situations of different effective local temperatures. This leads to both nonequilibrium effect from difference in accelerations or equivalent space time curvatures and distance effect on the quantum correlations between the two detectors.

Our paper is organized as follows. In Sec. II we review the continuous-variable techniques introduced in Ref. [22] which holds for an arbitrary time dependent quadratic Hamiltonian and an arbitrary number of modes in stationary cavities. Based on this, we also quantify the correlation measures (the logarithmic negativity as a measure of entanglement, the mutual information, and the Gaussian quantum discord) between the two detectors. In Sec. III we will present our main results. We have considered different scenarios for the two detectors: both stationary, both accelerated, accelerated in the same direction and opposing direction, equilibrium detectors with equal accelerations and nonequilibrium detectors with different accelerations or different couplings to the vacuum field under the same accelerations. We provided detailed discussions. In Sec. IV we give the conclusion.

## II. Calculation Method and Formalism

### 1. Time evolution of the operators:

Let us consider the global Hamiltonian and discuss how the dynamics evolves with respect to the proper time of an arbitrary detector. Throughout this paper we will use the conventions with  $c = \hbar = k_B = 1$ . Consider a general time dependent Hamiltonian  $\hat{H}(t)$ , where  $t$  is the global time coordinate. The Heisenberg equation of motion of a general operator  $\hat{A}(t)$  is then given by

$$\frac{d}{dt}\hat{A}(t) = i[\hat{H}(t), \hat{A}(t)] + \frac{\partial \hat{A}(t)}{\partial t} \quad (1)$$

Another coordinate choice is the local proper time  $\tau_j$  which corresponds to the world line  $(t(\tau_j), x(\tau_j))$  traversed by detector  $j$  at  $x$  and  $t$ . Applying the chain rule, the two time coordinates are associated,

$$\begin{aligned} \frac{d}{d\tau_j}\hat{A}[t(\tau_j)] &= \frac{dt}{d\tau_j} \frac{d}{dt}\hat{A}(t)|_{t=t(\tau_j)} \\ &= \frac{dt}{d\tau_j} \left\{ i[\hat{H}(t), \hat{A}(t)] + \frac{\partial \hat{A}(t)}{\partial t} \right\} \\ &= i \left[ \frac{dt}{d\tau_j} \hat{H}[t(\tau_j)], \hat{A}[t(\tau_j)] \right] + \frac{\partial \hat{A}[t(\tau_j)]}{\partial \tau_j} \end{aligned} \quad (2)$$

We can rewrite the Hamiltonian as

$$\hat{H}_j(\tau_j) := \frac{dt}{d\tau_j} \hat{H}[t(\tau_j)] \quad (3)$$

This is the Hamiltonian seen by  $j$ th detector. Therefore, we can provide a table for transformation to any other time coordinate. In fact  $\frac{dt}{d\tau_j}$  is the redshift factor for an observer in

the detector's reference frame. It provides an overall scaling of all energies in the whole system since this is what such an observer would experience. For the corresponding form, let us define

$$\hat{A}_j(\tau_j) := \hat{A}[t(\tau_j)] \quad (4)$$

We can use Eqs. (3) and (4) to rewrite Eq. (2) for the evolution dynamics of the operator as

$$\frac{d}{d\tau_j} \hat{A}_j(\tau_j) = i[\hat{H}_j(\tau_j), \hat{A}_j(\tau_j)] + \frac{\partial \hat{A}_j(\tau_j)}{\partial \tau_j} \quad (5)$$

## 2. Hamiltonian of the detector, field and detector-field interactions

We will study the interaction of a number of particle detectors coupled with a quantum massless scalar field. Let us consider an  $X-X$  coupling form of the Unruh-DeWitt Hamiltonian.[11-13] A general form of the Unruh-DeWitt detector field interaction is given by

$$\hat{H}_1 = \lambda(\tau) \hat{\mu} \hat{\phi}[x(\tau)] \quad (6)$$

where  $\lambda(\tau)$  is the switching function or coupling,  $\hat{\mu}$  is the monopole moment of the detector and  $\hat{\phi}[x(\tau)]$  is the scalar field operator evolving along the worldline of the detector parametrized in terms of the proper time  $\tau$ . Here, the subscript "1" of the Hamiltonian represents the interaction term and the subscript "0" of the Hamiltonian represents the free Hamiltonian term. To derive the correct form of the Hamiltonian in the Heisenberg pictures, let us first write the field and monopole operators in the Schrödinger picture. For clarity, we first consider just one detector undergoing general motion in flat space time with an associated proper time  $\tau$  with a scalar quantum field expand in terms of the plane wave solutions:

$$\hat{\phi}^S[x(\tau)] = \sum_n \hat{a}_n v_n[x(\tau)] + \hat{a}_n^\dagger v_n[x(\tau)] \quad (7)$$

Here, the superscript "S" denotes the Schrödinger picture. "H" denotes the Heisenberg picture.  $\hat{a}_n$  and  $\hat{a}_n^\dagger$  are the annihilation and creation operator for the  $n$ th field mode respectively.  $v_n$  is the spatial part of the  $n$ th mode solution to the field equations, i.e. the  $n$ th mode function. We consider the field and the detector are all in a stationary cavity in flat space time. In order to determine these mode functions, we need to impose boundary conditions for the cavity. For example, in the case of reflecting boundary conditions the mode function becomes

$v_n(x) = \frac{1}{\sqrt{k_n L}} \sin[k_n x]$ . Here  $k_n$  is the wave vector for the  $n$ th field mode. The mode function is given by

$$u_n(x, t) = \frac{1}{\sqrt{k_n L}} \exp(-i\omega_n t) \sin[k_n x] \quad (8)$$

under the reflecting boundary conditions. We will consider the reflecting boundary conditions in

our studies. For the massless scalar field,  $\omega_n = |k_n|$  and  $k_n = n\pi/L$  for the reflecting boundary conditions where  $L$  is the length of the cavity. The monopole moment of the detector  $\hat{\mu}$  in the Schrödinger picture is

$$\hat{\mu}^S = (\hat{a}_d + \hat{a}_d^\dagger) \quad (9)$$

where  $\hat{a}_d$  and  $\hat{a}_d^\dagger$  are the annihilation and creation operator respectively for the detector. Now, we write down the whole Hamiltonian  $\hat{H}^S$  in the Schrödinger picture with respect to the detector's proper time under transformation table as

$$\begin{aligned} \hat{H}^S(\tau) &= \hat{H}_0^S + \hat{H}_1^S \\ &= \frac{d\tau(\tau)}{d\tau} \sum_n \omega_n \hat{a}_n^\dagger \hat{a}_n + \Omega \hat{a}_d^\dagger \hat{a}_d + \lambda(\tau) (\hat{a}_d + \hat{a}_d^\dagger) \sum_n (\hat{a}_n v_n[x(\tau)] + \hat{a}_n^\dagger v_n[x(\tau)]) \end{aligned} \quad (10)$$

where  $\Omega$  is the characteristic frequency of the detector. The first terms of the above equation represent the Hamiltonian of the scalar field. The second term represents the Hamiltonian of the detector. The third terms represent the interactions between the field (modes) and the detector.

Notice that the form of the complete Hamiltonian in the Heisenberg picture coincides with the form of the Hamiltonian in the Schrödinger picture. It is straightforward to write the most general  $X-X$  type Hamiltonian for an arbitrary number of detectors undergoing general trajectories with different proper times  $\tau_j$  and with the time dependent couplings.

$$\begin{aligned} \hat{H}^H(t) &= \hat{H}_0^H + \hat{H}_1^H = \\ &= \sum_{n=1}^N \omega_n \hat{a}_n^\dagger \hat{a}_n + \sum_{j=1}^M \frac{d\tau_j}{dt} [\Omega_j \hat{a}_{d_j}^\dagger \hat{a}_{d_j} + \sum_{n=1}^N \lambda_{nj}(t) (\hat{a}_{d_j} + \hat{a}_{d_j}^\dagger) (\hat{a}_n v_n[x(\tau)] + \hat{a}_n^\dagger v_n[x(\tau)])] \end{aligned} \quad (11)$$

Here the first terms of the above equation represents the Hamiltonian of the scalar field. The second terms represent the Hamiltonian of the detectors. The third terms represent the interactions between the field (modes) and the detectors. From Eqs. (11), a natural IR cutoff of field modes is introduced due to our cavity setting with a length  $L$ . A UV cutoff is introduced for the sake of computation and resolution of the detectors.

### 3. Evolution dynamics of the detectors

Traditionally, two main approaches to quantum information processing have been pursued. [24] On the one hand, quantum information is encoded into the systems with a discrete, finite number of degrees of freedom such as qubits. Typical examples of qubit implementations are the nuclear spins of individual atoms in a molecule, the polarization of photons, ground/excited states of trapped ions, etc. On the other hand, a continuous approach has also been investigated. This is based on the quantum information and correlations encoded in the degrees of freedom through continuous variables. Typical examples of continuous variable implementations are position and momentum of a particle etc. In this study, we will mainly use the second approach. Specifically, both the detectors and the scalar field modes are described as continuous-variable to account the underlying bosonic degrees of freedom. We will use the Hamiltonian (11) in the

Heisenberg picture to evolve the quadrature operators  $(\hat{q}_{a_j}(t), \hat{p}_{a_j}(t))$  for each detector and  $(\hat{q}_n(t), \hat{p}_n(t))$  for each field mode, where  $j$  runs over all detectors and  $n$  for all field modes. These coordinate and momentum operators satisfy the standard canonical commutation relations as follows:  $[\hat{q}_{a_j}, \hat{p}_{a_i}] = i \delta_{ij}$ ,  $[\hat{q}_n, \hat{p}_k] = i \delta_{nk}$ . We organize these operators in a phase-space vector form as

$$\hat{X} := (\hat{q}_{a_1}, \hat{p}_{a_1}, \dots, \hat{q}_{a_j}, \hat{p}_{a_j}, \dots, \hat{q}_1, \hat{p}_1, \dots, \hat{q}_n, \hat{p}_n)^T \quad (12)$$

The vector  $\hat{X}$  in a phase-space naturally has a symplectic form  $[\hat{X}, \hat{X}^T] = i \Delta = i \oplus_i \begin{pmatrix} 0 & 1 \\ -1 & 0 \end{pmatrix}$ , where  $i$  runs through all degrees of freedom (both detectors and field modes). We will consider the state of our detector–field system to be a Gaussian states,[25] for a continuous variable ensemble. A Gaussian state is defined as any state whose characteristic functions and quasi-probability distributions are Gaussian functions in the quantum phase space. In general, a Gaussian state is fully characterized by its first and second canonical moments only.[24] In our study, a Hamiltonian that is quadratic in the operators with no linear terms as Eqs. (11) is considered. As a result, all states are Gaussian with no-displacement, and all evolutions are homogeneous Gaussian unitary. Therefore, we may neglect the first moments and the state is fully described by the second moments or the covariance matrix  $\sigma$ .

$$\sigma_{ij} = \langle \hat{x}_i \hat{x}_j + \hat{x}_j \hat{x}_i \rangle - 2\langle \hat{x}_i \rangle \langle \hat{x}_j \rangle \quad (13)$$

The time evolution of the entire covariance matrix, including both the detector and the field, is governed by the equation of unitary evolution

$$\sigma(t) = \mathbf{S}(t)\sigma(0)\mathbf{S}(t)^T \quad (14)$$

Here,  $\mathbf{S}$  is a symplectic matrix:  $\mathbf{S} \Delta \mathbf{S}^T = \mathbf{S}^T \Delta \mathbf{S} = \Delta$  and  $\hat{X}(t) = \mathbf{S}(t)\hat{X}(0)$ . In Hilbert space, the evolution of a state is dependent on time evolution operator  $\hat{U}$ ,  $\mathbf{S}$  plays the same role in the quantum phase space. A general time-dependent, quadratic, Heisenberg-picture Hamiltonian can be written as

$$\hat{H} = \hat{X}^T \mathbf{F}(t) \hat{X} \quad (15)$$

Here  $\mathbf{F}(t)$  is a Hermitian matrix of the c-numbers only determined by the explicit time-dependence of the Hamiltonian. For more details about deriving  $\mathbf{F}(t)$ , please see appendix. The Heisenberg equation for the time evolution of the quadratures is given by

$$\frac{d\hat{X}}{dt} = i[\hat{H}, \hat{X}] \quad (16)$$

Using Eqn.(15)(16) and definition of  $\Delta$ , one derives

$$\frac{d\hat{X}}{dt} = \Delta \mathbf{F}^{sys} \hat{X} \quad (17)$$

Here  $\mathbf{F}^{sys} = \mathbf{F} + \mathbf{F}^T$ . This is just the quantum phase space version of the Schrödinger equation. Using  $\hat{X}(t) = \mathbf{S}(t)\hat{X}(0)$  and  $[\hat{X}, \hat{X}^T] = i \Delta$ , finally we get

$$\frac{d}{dt} \mathbf{S}(t) = \Delta \mathbf{F}^{sys} \mathbf{S}(t) \quad (18)$$

Note that once we solve (18) with the initial condition  $\mathbf{S}(0) = \mathbf{I}$  such that  $\hat{X}(0) = \mathbf{S}(0)\hat{X}(0)$ , we know the evolution of the detectors–field system. In the particular simple cases where the Hamiltonian at different times commute, the solution of (18) can be obtained analytically and it is simply  $\mathbf{S}(t) = \mathbf{exp}[\Delta \mathbf{F}^{sys} t]$ .

### III. Result

#### 1. Quantum correlation measures: entanglement, mutual information and discord

##### A. Covariance and S matrix evolution

In what follows, we will consider two accelerated detectors which are moving inside a stationary cavity in flat space-time. The two separable detectors are initially stationary inside the cavity. The detectors are made as harmonic oscillator rather than a qubit. They both have the same characteristic frequency  $\Omega$ . We focus on the one dimensional dynamics, so we choose a smooth cavity with length  $L$ , and impose a reflecting boundary leading to the null field modes on the boundary. Therefore, there is a natural IR cutoff for the field modes A UV cutoff is introduced for the sake of computation and resolution of detectors. The Hamiltonian reads

$$\begin{aligned} \hat{H}^{\text{accelerated}}(t) = & \\ & \sum_{n=1}^N \omega_n \hat{a}_n^\dagger \hat{a}_n + \sum_{j=1}^2 \frac{d\tau_j}{dt} [\Omega \hat{a}_{d_j}^\dagger \hat{a}_{d_j} + \\ & \sum_{n=1}^N \lambda_{nj}(t) (\hat{a}_{d_j} + \hat{a}_{d_j}^\dagger) (\hat{a}_n v_n[x_j(\tau)] + \hat{a}_n^\dagger v_n[x_j(\tau)])] \quad (19) \end{aligned}$$

$$\begin{aligned} \hat{H}^{\text{stationary}}(t) = & \\ & \sum_{n=1}^N \omega_n \hat{a}_n^\dagger \hat{a}_n + \sum_{j=1}^2 [\Omega \hat{a}_{d_j}^\dagger \hat{a}_{d_j} + \sum_{n=1}^N \lambda_{nj}(t) (\hat{a}_{d_j} + \hat{a}_{d_j}^\dagger) (\hat{a}_n v_n[x_j(\tau)] + \hat{a}_n^\dagger v_n[x_j(\tau)])] \quad (20) \end{aligned}$$

From the above Hamiltonian,  $\mathbf{F}^{sys}$  can be derived. From Eqs.(18):  $\frac{d}{dt} \mathbf{S}(t) = \Delta \mathbf{F}^{sys} \mathbf{S}(t)$ , we can calculate the evolution of the symplectic matrix  $\mathbf{S}(t)$ .

An accelerated detector will experience a thermal bath in which the temperature is associated by  $T = \frac{a}{2\pi}$ , where  $a$  is the proper acceleration of the detector. The initial continuous

variables for covariance read

$$\boldsymbol{\sigma}_f^0 = \mathbf{I}_{2N} \quad (21)$$

$$\text{or } \boldsymbol{\sigma}_f^0 = \bigoplus_i \begin{pmatrix} v_i & 0 \\ 0 & v_i \end{pmatrix} \quad (22)$$

Eqns.(21) denotes a field at vacuum state and Eqns.(22) denotes a field at thermal state, where  $v_i = \frac{\exp(\frac{\omega_i}{T})+1}{\exp(\frac{\omega_i}{T})-1}$ , where  $T$  is the temperature of the field.[14]

$$\boldsymbol{\sigma}_d^0 = \mathbf{I}_4 \quad (23)$$

Eqn(23) is for both accelerated and stationary detectors. The initial continuous covariance matrix of the whole system is given as

$$\boldsymbol{\sigma}(0) = \boldsymbol{\sigma}_f^0 \oplus \boldsymbol{\sigma}_d^0 \quad (24)$$

Once determined from the Eqns.(14)  $\boldsymbol{\sigma}(t) = \mathbf{S}(t)\boldsymbol{\sigma}(0)\mathbf{S}(t)^T$ , the covariance matrix evolution of our system can be obtained and will take the generic form

$$\boldsymbol{\sigma}(t) = \begin{pmatrix} \boldsymbol{\sigma}_d & \boldsymbol{\gamma} \\ \boldsymbol{\gamma}^T & \boldsymbol{\sigma}_f \end{pmatrix} \quad (25)$$

Here  $\boldsymbol{\sigma}_d$  and  $\boldsymbol{\sigma}_f$  represent the  $4M \times 4M$  and  $4N \times 4N$  covariance matrices of the reduced states of the  $M$  detectors and  $N$  field modes, respectively. The matrix  $\boldsymbol{\gamma}$  contains the information regarding correlations between the detectors and the field. We can compute the correlation measures between the detectors such as the logarithmic negativity for entanglement, the mutual information, and quantum discord. The covariance matrix of the detector-detector state that we obtain upon evolution will be in the generic form (only consider the two detectors case)

$$\boldsymbol{\sigma}_d = \begin{pmatrix} \boldsymbol{\sigma}_{d_1} & \boldsymbol{\gamma}_{12} \\ \boldsymbol{\gamma}_{12}^T & \boldsymbol{\sigma}_{d_2} \end{pmatrix} \quad (26)$$

As in Eqns.(26),  $\boldsymbol{\sigma}_{d_1}$  and  $\boldsymbol{\sigma}_{d_2}$  describe the reduced states of detectors 1 and 2. The matrix  $\boldsymbol{\gamma}_{12}$  stores information regarding the correlations between the two detectors. As an example, the detectors will be uncorrelated (i.e., in a product state) if and only if all entries of  $\boldsymbol{\gamma}_{12}$  are zero.

## B. Quantum Correlations: entropy, entanglement, mutual information and discord

The Von Neumann entropy of a general Gaussian state can be given by [23]

$$S_{VN}(\boldsymbol{\sigma}) = \sum_{i=1}^N s(v_i) \quad (27)$$

$$s(x) = \frac{x+1}{2} \log_2 \left( \frac{x+1}{2} \right) - \frac{x-1}{2} \log_2 \left( \frac{x-1}{2} \right) \quad (28)$$

Here  $v_i$  is the  $i$ th symplectic eigenvalue.(i.e. the orthogonal eigenvalues of the matrix  $|i \Delta \boldsymbol{\sigma}|$ )

The mutual information between the detectors, which quantifies the total amount of correlation between the subsystems that can potentially be useful for computational tasks, then follows the usual form [6],

$$I = S_{VN}(\sigma_{d_1}) + S_{VN}(\sigma_{d_2}) - S_{VN}(\sigma_d) \quad (29)$$

It is easy to see when  $\gamma_{12} = 0$ ,  $I = 0$ , and there is no correlation between the two detectors. Define the quantities  $\alpha = \text{Det}[\sigma_{d_1}]$ ,  $\beta = \text{Det}[\sigma_{d_2}]$ ,  $\gamma = \text{Det}[\gamma_{12}]$  and  $\delta = \text{Det}[\sigma_d]$ , then the logarithmic negativity for characterizing the entanglement between the detectors is given as [23]

$$E_N = \text{Max}\{0, -\log_2 \tilde{v}_-\} \quad (30)$$

where  $\tilde{v}_-$  is the smaller of the state's partially transposed symplectic eigenvalues which is given

$$\text{by } \tilde{v}_- = \sqrt{\frac{\tilde{\Delta} - \sqrt{\tilde{\Delta}^2 - 4\delta}}{2}}, \text{ where } \tilde{\Delta} = \alpha + \beta - 2\gamma.$$

The quantum discord is a measure of the pure quantum part of correlations obtained by subtracting off the classical correlations from the mutual information. It is a measure of the information that cannot be extracted without joint measurements. The discord is a good indicator of quantum nature of quantum correlation.[5] It is given by [26]

$$D(1:2) = s(\sqrt{\beta}) - s(\sqrt{v_1}) - s(\sqrt{v_2}) + s(\sqrt{E}) \quad (31)$$

where  $v_1$  and  $v_2$  are the symplectic eigenvalues of  $\sigma_d$  and  $E$  is defined as

$$E = \begin{cases} \frac{2\gamma^2 + (-1+\beta)(-\alpha+\beta) + 2|\gamma|\sqrt{\gamma^2 + (-1+\beta)(-\alpha+\beta)}}{(-1+\beta)^2} \\ \text{for } (-\alpha\beta + \delta)^2 \leq (-1 + \beta)(\alpha + \delta)\gamma^2 \\ \frac{\alpha\beta - \gamma^2 + \delta - \sqrt{\gamma^4 + (-\alpha\beta + \delta)^2 - 2\gamma^2(\alpha\beta + \delta)}}{2\beta} \\ \text{otherwise} \end{cases} \quad (32)$$

In general, the discord is not symmetric  $D(1:2) \neq D(2:1)$ .

## 2. Equilibrium Quantum Correlations Between the Two Equally Accelerated Detectors

### A. Accelerations of the Detectors in the Same Direction

#### 1) Entanglement

In what follows, we will consider the two detectors which are in the equilibrium state. This means that they are either stationary and have the same temperature or have the same

accelerated motion in the cavity. The world line can be given by  $(t, \pi, 0, 0)$  and  $(t, 2\pi, 0, 0)$  for the two stationary detectors named as Alex and Rob while  $(a^{-1} \sinh(a\tau), a^{-1}(\cosh(a\tau) - 1), 0, 0)$  and  $(a^{-1} \sinh(a\tau), a^{-1}(\cosh(a\tau) - 1 + a\pi), 0, 0)$  for the two accelerated detectors Alice and Bob respectively. We have several setups for considerations: a) two detectors accelerate with the same acceleration while they start from the vacuum state; b) two separated detectors start at vacuum state initially and then stationary immersed in a thermal field. We are interested in exploring the behaviors of entanglement, mutual information and quantum discord between detectors from the field in different setting.

The logarithmic negativity  $E_N$  between the detectors is a measure of entanglement. We show this entanglement measure in two cases in Figure (1a)(1b), Figure (1a) depicts  $E_N$  between the two accelerated detectors varying with the acceleration and the time. Figure (1b) depicts  $E_N$  between the two stationary detectors varying with respect to the temperature of field and the time.

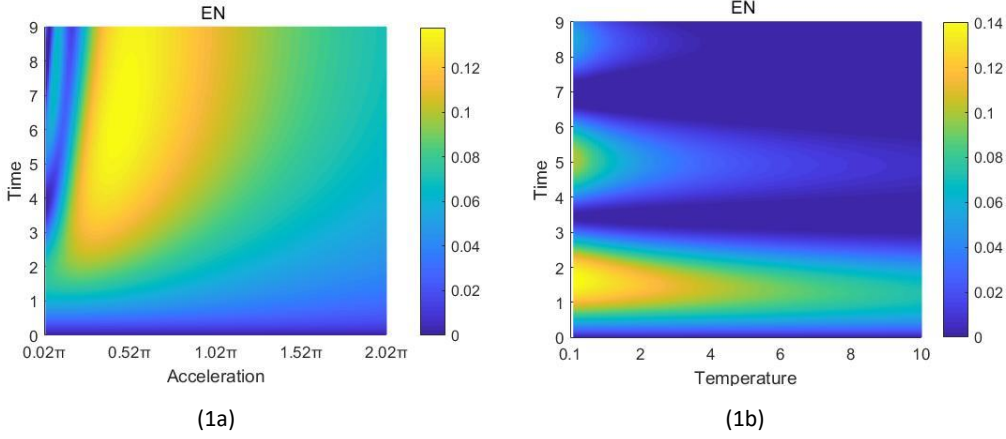


Figure (1a) describes how  $E_N$  varies with respect to the acceleration and the time. One starts from a lower acceleration  $0.02\pi$ , while the two detectors accelerate with the same proper acceleration and always stay at a distance  $\pi$  from each other. Figure (1b) describes how  $E_N$  varies with respect to the temperature of the field and time. One starts from a lower temperature  $0.01$ , while the two detectors are stationary at a distance  $\pi$  from each other. The acceleration corresponds to the temperature from Unruh effect  $T = \frac{a}{2\pi}$ . The cavity length is  $4\pi$ , while the detector's response frequency is set as  $\Omega = \frac{3}{2}$ , which indicates that the detector is in resonance with the 6th field mode. The number of field modes is set as 18, and the coupling strength for both detectors is set as  $\lambda = 0.05$ .

We found that the two detectors initially unrelated can harvest the entanglement from the field. When the acceleration or temperature is low, the trend of entanglement over time for acceleration and temperature is very similar: there are several ups and downs over time, but they all tend to gradually decrease in a fluctuating way. The reason of the similarity is as follows: the two accelerated detectors at the low accelerations will only have effective low local temperatures near the detector sites due to the Unruh effect. They are coupled by the vacuum field. On the other hand, the two stationary detectors at the low temperature also have local thermal environments with the vacuum field as the bridge between them. When the coupling field becomes thermal, the field is still very vacuum-like under low temperatures. Therefore at the low temperature or acceleration, the entanglements for temperature and acceleration have similar

behavior. This shows the similarities between the two.

We can also explain the difference between the entanglements at low acceleration and low temperature: the thermal baths experienced by the accelerated detectors are locally distributed and their characteristic frequencies are redshifted. In details, due to the accelerated motion, the intrinsic frequency of the detector oscillator  $\Omega$  is redshifted by the factor  $\frac{d\tau}{dt}$  which leads  $\Omega$  to be increasingly smaller as time goes on.

The possible explanation for the fluctuating oscillation pattern in time of the entanglement might be the quantum recurrence (live and die) behavior from the non-Markovian effect[27]. The fluctuating decrease behavior of the entanglement may come from the fact that at long times the systems reaches equilibrium and thermal mixed state which is lack of the quantum nature.

At a higher temperature of the detectors,  $E_N$  still decreases in a fluctuating way over time and finally vanishes. This is similar to the above situation when the temperature is low which can be explained by the same physical reason. The oscillation of the entanglement in time may be from the quantum recurrence while the fluctuating decrease of entanglement may come from the long time thermal equilibrium mixed state.

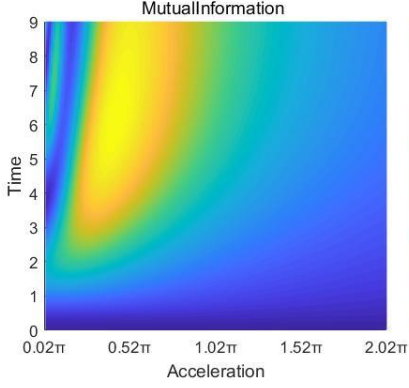
At fixed times, as the temperature increases, the entanglement decreases monotonically. When the temperature is high enough, there is no entanglement in Figure (1b). As the temperature increases, the quantum effects become less compared to the thermal effects with the classical nature. At the very high temperature, the thermal nature overwhelms the quantum nature. This may explain the downward trend of the entanglement at fixed times when the temperature increases.

For the case under larger acceleration, the entanglement  $E_N$  can increase over time until reaching a constant in Figure(1a) from  $0.2\pi$  to  $2.02\pi$ . This is because the characteristic frequency of the accelerated detector is redshifted and the corresponding response period is elongated. Finite time is considered in this case due to the fact that detectors are contained in a cavity.

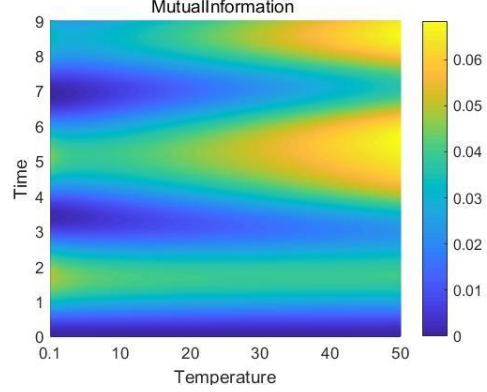
At fixed times, as acceleration increases the entanglement first increases and then decreases. The local acceleration by equivalence principle is equivalent to the local gravity. According to the general relativity, the local gravitational field can lead to a redshift in radiation frequency. Therefore, the characteristic frequency of the detector under acceleration is redshifted and the associated time is elongated. This leads to the widening of the high entanglement band at the same acceleration as seen in Figure 1a. Furthermore, the higher acceleration will result to lower frequency due to the redshift effect and more elongated times. This leads the high entanglement band to be titled as observed in Figure 1a. Therefore, at fixed times, the entanglement will meet the high entanglement band as the acceleration initially increases. Thus, the acceleration induced redshift is the cause for the initial increase of the entanglement at fixed times. As the acceleration or the associated Unruh temperature further increases, the local thermal fluctuations will eventually lead to the more classical mixed state behavior and be more harmful for the quantum nature such as entanglement. This results to the downward trend of the entanglement at fixed times beyond certain acceleration values.

## 2) Quantum Mutual Information and Quantum Discord

The mutual information between the two detectors, which quantifies the total quantum correlation, is shown in Figure (2a)(2b). In our setting, the quantum mutual information has almost the same trend in time and acceleration (temperature) compared to the quantum discord, for the sake of simplicity, we just consider the quantum discord in details. The statement also holds for mutual Information.



(2a)



(2b)

Figure (2a) describes how mutual information varies with respect to the acceleration and time. One starts from a lower acceleration  $0.02\pi$ , while the two detectors accelerate with the same proper acceleration and are at a distance  $\pi$  from each other. Figure (2b) describes how the mutual information varies with respect to the temperature of field and the time. One starts from a lower temperature  $0.01$ , while the two detectors are stationary at a distance  $\pi$  from each other. All parameters are the same as those in Figure (1).

We plot in Figure.(3a)(3b) the quantum discord between the detectors in the same scenario as Figure.(2a)(2b). Quantum discord is a measure of the pure quantum part of the correlations obtained by subtracting off the classical correlations from the quantum mutual information. The trend in Figure (3a)(3b) for quantum discord are very similar to that for quantum mutual information in Figure (2a)(2b). The quantum discord (mutual information) varies with acceleration and time or temperature and time, their behaviors are quite similar to that of the entanglement  $E_N$ . This can follow the same explanation on the entanglement of  $E_N$ . The only difference is that the quantum discord (mutual information) is amplified by the higher temperature rather than being reduced as in the case of entanglement.

At higher temperatures, the quantum discord (mutual information) is more robust than the entanglement  $E_N$ . Moreover, as the temperature of the stationary detectors increases, quantum discord can be amplified via increasing the temperature which was suggested in Ref[23]. The entanglement and quantum discord has a monogamic relationship in a tripartite system (two subsystems in an environment)[28]. Moreover, Ref[29] shows that the evolution of the discord reflects the entanglement entropy dynamics between the system and the environment, and its behavior is opposite to the entanglement between the (sub)systems. This implies that increasing the temperature of the field can lead the detectors to be more mixed and therefore more likely

to be entangled with the environment in our case. This leads to an increased amount of discord (mutual information) but less entanglement between the detectors.

Unlike entanglement  $E_N$ , the quantum discord (mutual information) may exist for long and still fluctuate over time in Figure(2b). We suggest that the evolution of quantum discord (mutual information) in such systems can be understood as a competition between the decoherence effect among the systems due to the environment (field) and the system-environment (detectors-field) entanglement that such decoherence also tends to generate. As we have seen, in this case the latter wins. The quantum discord is sustained due to the dominant system-environment (detector-field) entanglement over the decoherence or the disentanglement from the system (detector-detector). On the other hand, the system-environment entanglement does not boost the entanglement within or between the systems. Indeed, due to monogamy, the entanglement is usually further damaged and therefore easier to be destroyed as shown in Figure 1b.

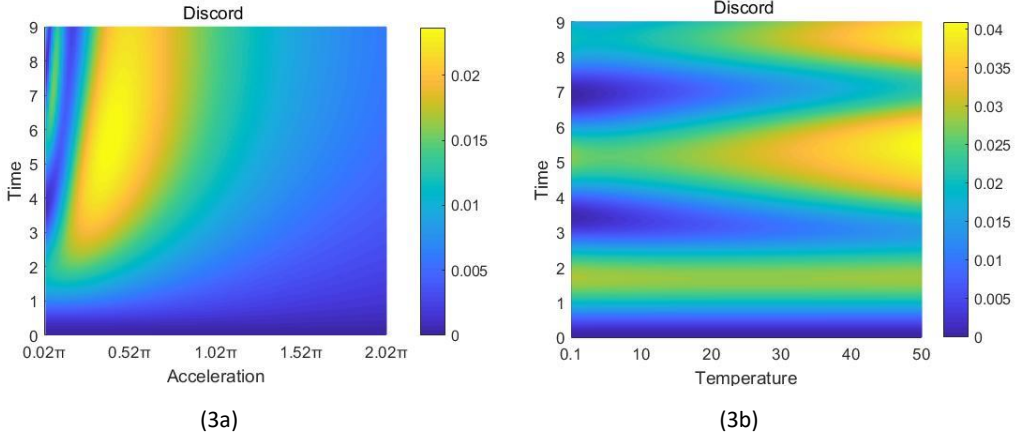


Figure (3a) describes how quantum discord varies with respect to the acceleration and the time. One starts from a lower acceleration  $0.02\pi$ , while the two detectors accelerate with the same proper acceleration and are at a distance  $\pi$  from each other. Figure (3b) describes how quantum discord varies with respect to the temperature and the time. One starts from a lower temperature 0.01, while the two detectors are stationary at a distance  $\pi$  from each other. All parameters are the same as those in Figure (1a) (1b).

When a detector is accelerated in flat space time, it will experience a thermal bath around. The bath effect can be viewed as the detector pumping energy into the field during the acceleration process, so the bath is local. From the above analysis, we learn that when the two detectors move in the same direction with the same acceleration at a constant distance, the entanglement、 mutual information and discord act like the stationary ones coupled to a thermal bath when the temperature or the acceleration is low. However, the quantum correlations such as entanglement, quantum mutual information and quantum discord between accelerated detectors behave differently from the stationary ones coupled to a thermal bath at higher temperature or acceleration.

Here we can see a significant difference between the effects of temperature of the flat space and effects of the space time through the corresponding acceleration on the entanglement, quantum mutual information and quantum discord. We can see that although Unruh and Hawking pointed out the equivalence of the temperature and the space-time geometry, they are only locally equivalent. The temperature and space-time show different impacts on the global correlations such as entanglement, mutual information and discord. As temperature increases, the entanglement decreases. However, as the acceleration increases or the effective space-time is more curved, the entanglement as well as the quantum mutual information and quantum discord can be increased. In other words, the more curved space can boost the quantum correlations. Since the curved space-time can shorten the effective distance and give rise to short cut(such as the wormhole), this may be the physical reason why the quantum correlation can be enhanced due to the space-time short cut. It might also give an explanation of the quantum non-locality from the curved space-time perspective. The actual effective distance through the short cut can be much shorter than the appeared one.

## B. Accelerations of the Detectors in the Opposite Directions

We now investigate the entanglement, the quantum mutual information and the quantum discord between the two accelerated detectors in the opposing direction. The world line are  $(a^{-1} \sinh(a\tau), a^{-1} (\cosh(a\tau) - 1 + 2a\pi), 0, 0)$  and  $(a^{-1} \sinh(a\tau), -a^{-1} (\cosh(a\tau) - 1 - 2a\pi), 0, 0)$  for Alice and Bob respectively. This mimics the two heat sources in flat space time moving away from each other. From Figure 4, as time goes on, Bob and Alice become further apart leading to less correlation than the case of the two accelerated detectors in the same direction. When the acceleration is relatively low, the entanglement, the quantum mutual information and the quantum discord between the two accelerated detectors increase firstly and then decrease, thereafter disappear for a while and then survive again in time from  $0.01\pi$  to  $0.12\pi$  in acceleration. The reason for the initial increase is from the interactions between the detectors and the field which lead to the harvest quantum correlations from the field. As time goes by, the detectors become further and further apart due to the opposite accelerations which lead to the decreasing correlations. Furthermore, the detector's characteristic frequency decreases from the redshift. In addition, the local thermal fluctuations are harmful for the quantum correlation. As the acceleration increases, the detectors become more separable at an instant, then the entanglement, the quantum mutual information and the quantum discord all decrease. However, the reduction rates are different. The reduction rate of the entanglement  $E_N$  is the smallest. Therefore, the entanglement  $E_N$  seems to be more robust than the quantum mutual information and the quantum discord at a longer distance.

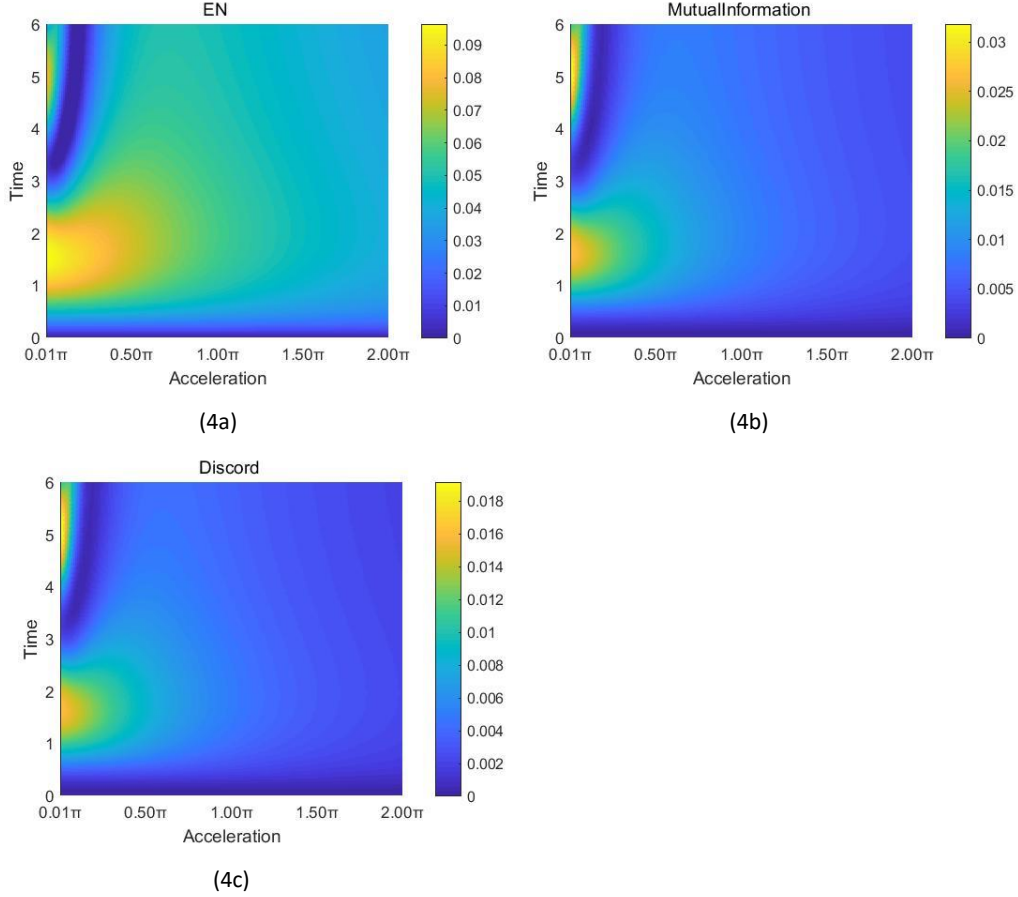


Figure (4a) describes how entanglement  $E_N$  varies with respect to the acceleration and time. One starts from a lower acceleration  $0.02\pi$  and the two detectors accelerate with the same proper acceleration in two opposing directions starting at  $2\pi$ . Figure (4b) describes how quantum mutual information varies with respect to the acceleration and time. One starts from a lower acceleration  $0.02\pi$ , and the two detectors accelerate with the same proper acceleration in two opposing directions starting at  $2\pi$ . Figure (4c) describes how the quantum discord varies with respect to the acceleration and time. One starts from a lower acceleration  $0.02\pi$ , and the two detectors accelerate with the same proper acceleration in two opposing directions starting at  $2\pi$ . All parameters are the same as those in Figure (1a) (1b).

### 3. Nonequilibrium Quantum Correlations Between the Two Different Accelerated Detectors

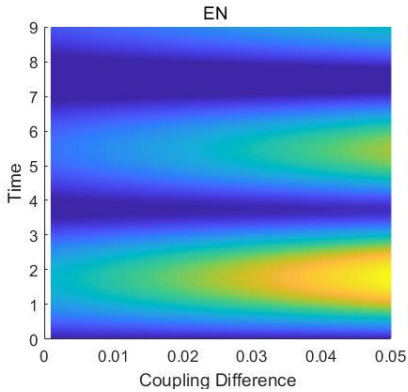
#### A. Nonequilibrium Quantum Correlations Between the Equally Accelerated Detectors from the Coupling Differences to the Scalar Field

##### 1) Quantum Entanglement

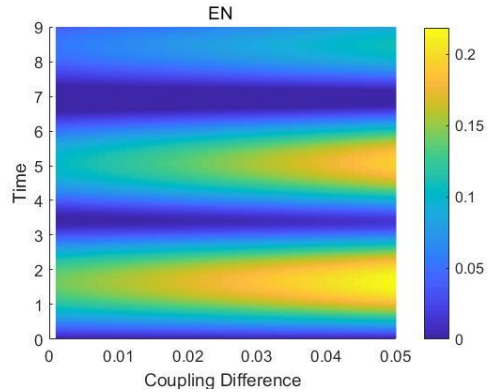
In this part, we will consider a nonequilibrium case with the coupling strengths between each detector and the scalar field in the cavity being different from another. The nonequilibriumness is characterized by the degree of the detailed balance breaking due to the different couplings of the detectors to the vacuum field. One can understand it this way, if the

two detectors are with different accelerations, then according to the Unruh effects, the two detectors are surrounded by the environments with different temperatures. The temperature difference creates the nonequilibrium condition. On the other hand, if the couplings of the accelerated detectors to the scalar field are different, then the occupation or the number density for the detectors would be different for the two detectors since they are not only dependent on the local temperatures but also on the couplings to the scalar field. This also creates an imbalance or nonequilibrium condition. We first consider the quantum correlations in the different coupling case with equal acceleration since we would like to separate the pure effects of the nonequilibriumness from that of the increased distance due to the accelerations. The world line is given as  $(t, \pi, 0, 0)$  and  $(t, 2\pi, 0, 0)$  for the two stationary detectors Alex and Rob respectively, while  $(a^{-1} \sinh(a\tau), a^{-1} (\cosh(a\tau) - 1), 0, 0)$  and  $(a^{-1} \sinh(a\tau), a^{-1} (\cosh(a\tau) - 1 + \pi), 0, 0)$  for the two accelerated detectors Alice and Bob respectively.

When the acceleration or the temperature is low, the stationary and accelerated ones behave similarly. The entanglement has several ups and downs as shown in Figure (5a)(5b) in time. The entanglement  $E_N$  is enhanced by increasing coupling constant. A larger coupling constant difference gives rise to a greater ability to harvest correlations from the field. As acceleration is larger, the entanglement at large acceleration behaves very differently from that at small acceleration with respect to the coupling difference at certain fixed time as shown in Figure (5c). In Figure (5c), the stripe is enlarged by the redshift effect. On the other hand, at the fixed coupling difference, the entanglement  $E_N$  decreases over time in Figure (5a) for small accelerated detectors while increases over time in Figure (5c) for large accelerated detectors. The behavior of the entanglement in Figure (5a) might be due to the thermalization in the long time. The behavior of the entanglement in Figure (5c) could be due to the fact that the large entanglement region is enlarged by the nonequilibrium effect from the imbalance or the difference in the two coupling constants of the detectors to their corresponding baths (more detailed discussions on this are given at the end of this subsection A) and the redshift effect. At the fixed coupling difference, the entanglement  $E_N$  decreases over time in Figure (5b)(5d) for stationary detectors. The entanglement within the system is not boosted by the system-environment entanglement. Indeed, it will generally be further impaired due to monogamy, and will therefore be far more easily destroyed.



(5a)



(5b)

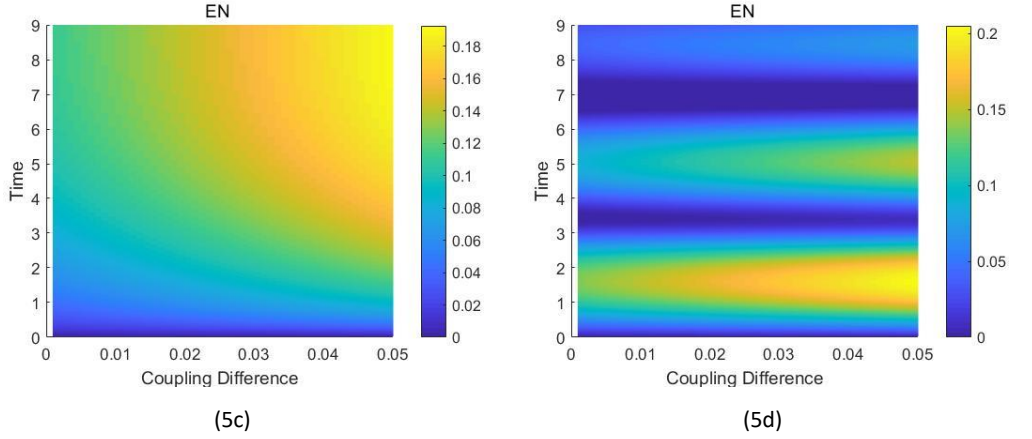
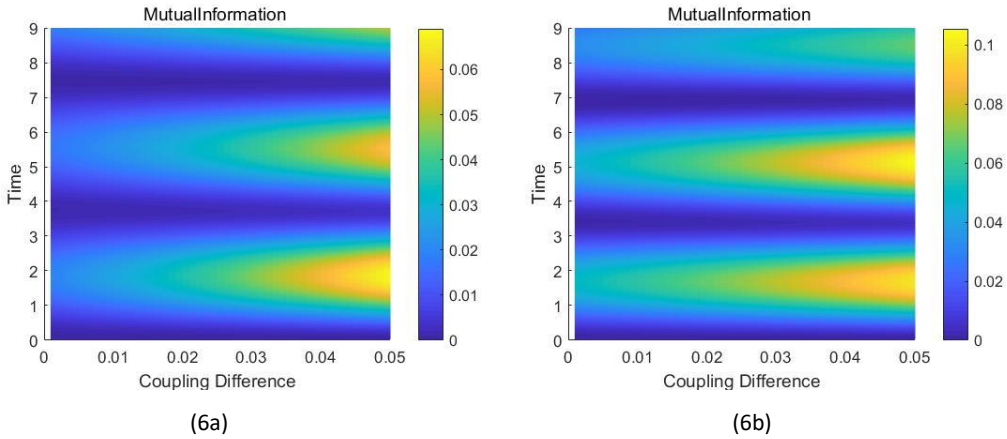


Figure (5a) describes how  $E_N$  varies with respect to the coupling difference and time. Alice and Bob stay at a lower constant proper acceleration  $0.02\pi$ , and at a distance  $\pi$  apart. Figure (5b) describes how  $E_N$  varies with respect to the coupling difference and time. Alex and Rob are stationary at thermal equilibrium at lower temperature  $0.01$  and also stay a distance  $\pi$  apart. Figure (5c) describes how  $E_N$  varies with respect to the coupling difference and time. Alice and Bob stay at a higher constant proper acceleration  $1.02\pi$ , and at a distance  $\pi$  apart. Figure (5d) describes how  $E_N$  varies with respect to the coupling difference and time. Alex and Rob are stationary at thermal equilibrium at higher temperature  $0.51$ . All the other parameters are the same as those in Figure (1).

## 2) Quantum Mutual Information and Quantum Discord

We depict how the quantum mutual information varies with respect to the coupling difference and time at different temperatures and different acceleration in (6a)(6b)(6c)(6d). In our setting, we find that the quantum mutual information has almost the same trend compared to the quantum discord. For the sake of simplicity, we will only discuss the quantum discord in details, the statement also holds for quantum mutual information.



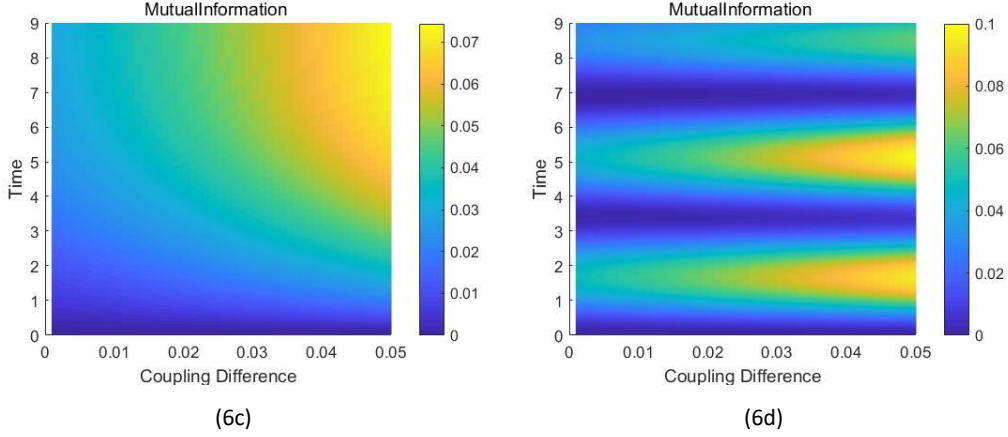


Figure (6a) describes how quantum mutual information varies with respect to the coupling difference and time. Alice and Bob stay at a lower constant proper acceleration  $0.02\pi$  and at a distance  $\pi$  apart. Figure (6b) describes how quantum mutual information varies with respect to the coupling difference and time. Alex and Rob are stationary in thermal equilibrium at lower temperature  $0.01$ . Figure (6c) describes how quantum mutual information varies with respect to the coupling difference and time. Alice and Bob stay at a higher constant proper acceleration  $1.02\pi$  and at a distance  $\pi$  apart. Figure (6d) describes how quantum mutual information varies with respect to coupling difference and time. Alex and Rob are stationary in thermal equilibrium at higher temperature  $0.51$ . All the other parameters are the same as those in Figure (1).

We depict how the quantum discord varies with respect to the coupling difference and time at different temperatures and different acceleration in (7a)(7b)(7c)(7d). Overall, the quantum discord (mutual information) behaves similarly as that of entanglement  $E_N$ . When the acceleration or temperature is low, stationary and accelerated ones act similarly. Quantum discord and mutual information will have several ups and downs as shown in Figure (6a, 7a)(6b, 7b) in time; The quantum discord and mutual information are enhanced by increasing coupling constant. A larger coupling constant difference gives rise to a greater ability to harvest correlations from the field. As acceleration is larger, the quantum discord and mutual information at large acceleration behaves very differently from that at small acceleration with respect to the coupling difference at certain fixed time as shown in Figure (6c, 7c). In Figure (6c, 7c), the stripes are enlarged by redshift effect. On the other hand, at the fixed coupling difference, the quantum discord and mutual information decrease over time in Figure (6a, 7a) for small accelerated detectors while increase over time in Figure (6c, 7c) for large accelerated detectors. The behavior of the quantum discord and mutual information in Figure (6a, 7a) might be due to the thermalization in the long time. The behavior of the quantum discord and mutual information in Figure (6c, 7c) are also due to the fact that the higher quantum discord and mutual information regions are enlarged by redshift effect.

At fixed coupling difference, the quantum discord and mutual information oscillate over time in Figure (6b, 7b)(6d, 7d). We suggest that the evolution of quantum discord in such systems can be understood as a competition between the decoherence effect among detectors from the environment (field) and the system-environment entanglement (detectors-field) closely associated with the quantum discord, in which such decoherence also tends to generate. As we have seen, here the detector-field entanglement becomes important and therefore the quantum discord or mutual information is sustained.

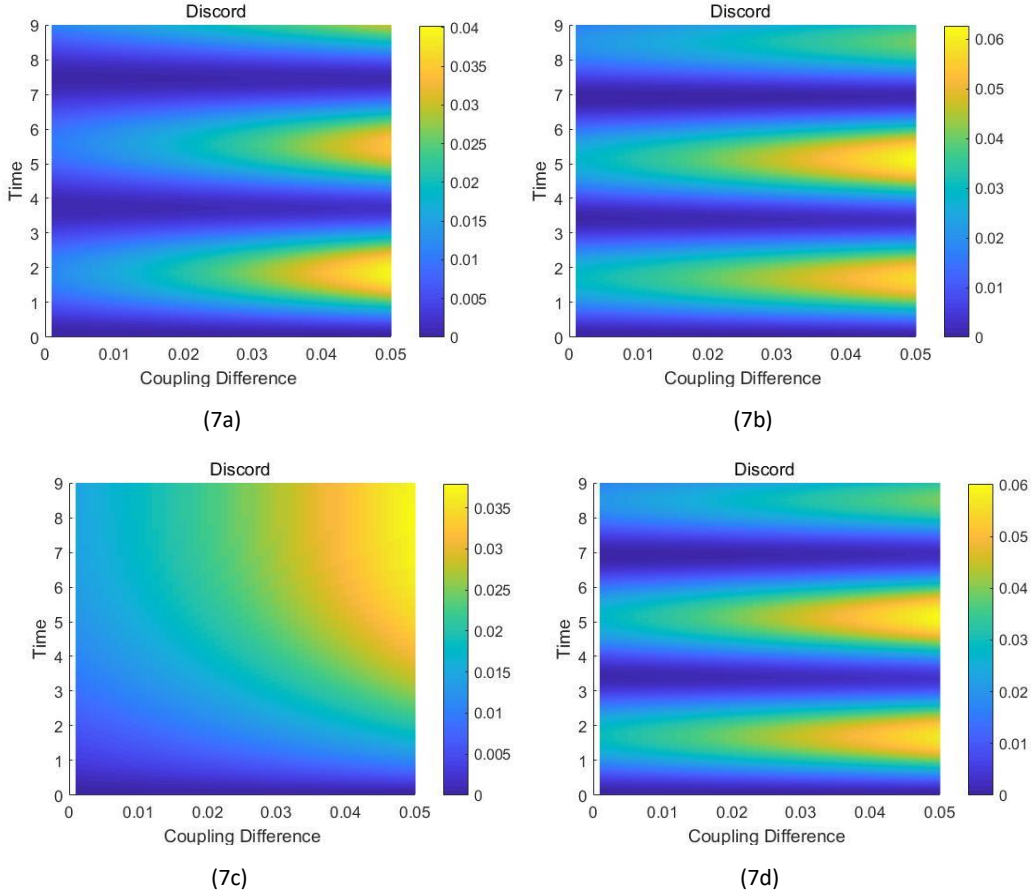


Figure (7a) describes quantum discord varies with respect to the coupling difference and time. Alice and Bob stay at a lower constant proper acceleration  $0.02\pi$  and at a distance  $\pi$  apart. Figure (7b) describes how quantum discord varies with respect to the coupling difference and time. Alex and Rob are stationary in thermal equilibrium at lower temperature 0.01. Figure (7c) describes how quantum discord varies with respect to the coupling difference and time. Alice and Bob stay at a higher constant proper acceleration  $1.02\pi$  and at a distance  $\pi$  apart. Figure (7d) describes quantum discord varies with respect to the coupling difference and time. Alex and Rob are stationary in thermal equilibrium at higher temperature 0.51. All the other parameters are the same as those in Figure (1).

Since the coupling difference of the system to the baths (two detectors coupled with the two different baths or the associate scalar field differently) can create an imbalance which leads to the net energy flow, this leads to the detailed balance breaking and generates the nonequilibriumness. The enhancement of the quantum correlations is apparent from the higher coupling difference or the nonequilibriumness when the underlying space time geometry is highly curved (higher local accelerations). In the previous section, we discussed how the local acceleration or the space-time geometry can enhance the quantum correlations. Here we see another source of the enhancement of the quantum correlations through the nonequilibriumness. The nature of the nonequilibriumness is from the net energy flow to the system. Since the mass and energy are equivalent with each other under the Einstein mass-energy relationship, the increase of the nonequilibriumness leads to the increase of the

energy flow and therefore the effective mass of the system. Since the local curvature of the space-time geometry is dependent on the mass of the system (such as the black hole), the increase of the nonequilibriumness can enhance the effective space-time curvature. An increased curvature can create space time fluctuations or short cut (such as wormhole) for traveling. This decreases significantly the effective distance for the communications. Thus one expects the nonequilibriumness can boost the quantum correlations through effectively enhancing the curvature of the space-time geometry or creating the space-time short cut.

## B. Nonequilibrium Quantum Correlations Between the Detectors with Different Accelerations

In this part, we will consider the case where the two detectors in the cavity are in nonequilibrium state with different accelerations. The world line is  $(a^{-1} \sinh(a\tau), a^{-1} (\cosh(a\tau) - 1), 0, 0)$  and  $(b^{-1} \sinh(b\tau), b^{-1} (\cosh(b\tau) - 1 + b\pi), 0, 0)$  for the two detectors Alice and Bob respectively.

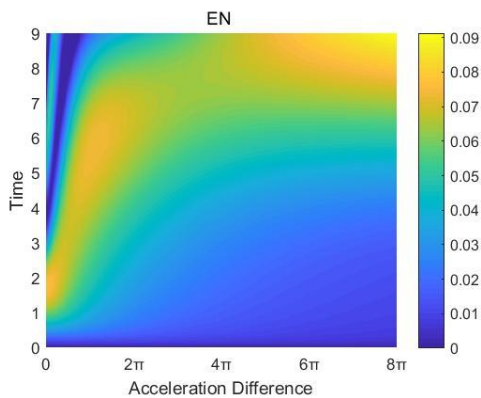
At low fixed acceleration differences in Figure (8a)(8b)(8c), the quantum information measures such as entanglement, mutual information and quantum discord exhibit up and down oscillations, and eventually decay in time. The possible explanation for these oscillation patterns in time may be from the quantum recurrence (live and die) behavior due to the non-Markovian effects[27]. The fluctuating decrease behavior of the quantum information may come from the fact that at long times the systems reaches the equilibrium and therefore is in the thermal mixed state lacking of the quantum nature.

At large fixed acceleration differences, the quantum information measures such as entanglement, mutual information and quantum discord increase as time goes by. This is because of the redshift effects. As shown in Figure (8a)(8b)(8c), at the small accelerations, we see periodic behaviors of the quantum information as time increases. The periodicity depends on the detector's response frequency  $\Omega$ . Due to accelerated motion, the intrinsic frequency of the detector oscillator  $\Omega$  is redshifted by the factor  $\frac{d\tau}{dt}$ . This leads to  $\Omega$  being increasingly smaller as time goes by. This means that it will take much longer time to have a period of oscillation compared to the smaller acceleration case with less redshifts and higher intrinsic detector response frequency. The enhancement or peak of the quantum correlations are therefore delayed in time for large acceleration difference case.

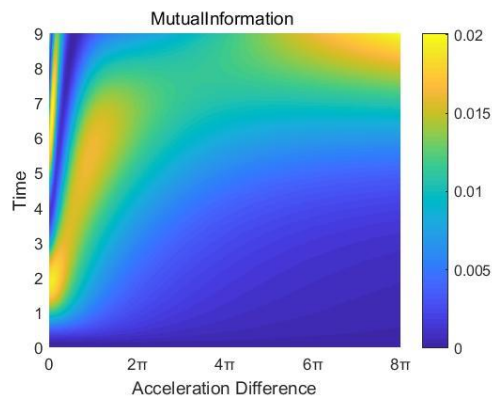
Unlike the equilibrium case, now the dynamics of the system is dominated by two distinct characteristic frequencies. As time goes by, the redshift effect is more significant. Due to the redshift, the corresponding response period is elongated and the maximum of the correlation harvesting from the scalar field is delayed. Therefore it appears that there are time regions in the pictures. At initial short times, the quantum measures such as entanglement, mutual information and quantum discord first increase and then decrease as the acceleration difference increases. If the acceleration of one detector is fixed while the other is allowed to vary, then as the acceleration of the detector increases, the characteristic frequency of the detector under accelerations is redshifted and the associated time is elongated. This results to the widening of the quantum correlation stripes for the same low acceleration differences as seen in Figure 8.

Increase further the acceleration will lead to longer elongated times. This leads the high quantum correlation stripes to be tilted as observed in Figure 8 in low acceleration differences. Thus, at fixed times, the quantum correlations will meet the high quantum correlation stripes as the acceleration difference initially increases. Thus, the acceleration induced redshift is the cause for the initial increase of the quantum correlations at the initial fixed times. In addition, the local thermal fluctuations can be harmful for the entanglement. This leads to the decay of the quantum correlations as the acceleration difference increases further.

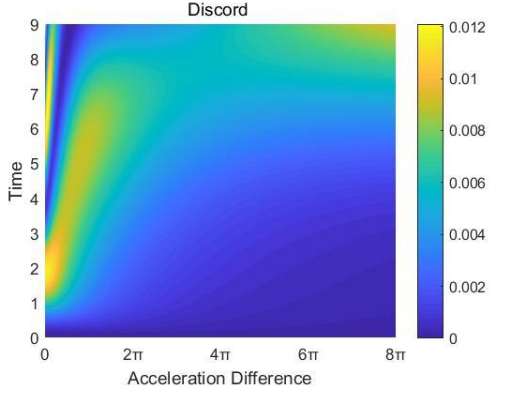
At the long time limit, the quantum measures such as entanglement, mutual information and quantum discord also first increase and then decrease. This is because there are two effects influencing the quantum correlations. The first one is the acceleration difference or the equivalently the effective Unruh temperature difference. The temperature difference can give rise to an imbalance which leads to the net energy flow. This destroys the detailed balance and creates the nonequilibriumness. The enhancement of the quantum correlations from the acceleration difference in Figure(8a)(8b)(8c) reflects the fact that the nonequilibriumness characterized by the degree of the detailed balance breaking can increase the quantum correlations. From the Einstein relationship of mass and energy, net energy flow is equivalent of a net mass gain. This can result in the more curved space time. A more curved space time can lead to a short cut for the space time distance. This can explain the increase of the correlations such as the entanglement, quantum discord and mutual information. Another effect is the distance one. It comes from the fact the two detectors in different accelerations increase their distances from each other. The larger distance will weaken the quantum correlations. The combination of the trend for increasing the quantum correlations from the nonequilibriumness and the trend for decreasing the quantum correlations due to the larger distances can give rise to the seemingly oscillatory pattern in quantum correlations at long times. The upward trend of the quantum correlations with respect to the increase of the acceleration difference is due to the nonequilibrium enhancement while the downward decrease trend of the quantum correlations with respect to the increase of the acceleration difference is due to the larger distances between the two detectors. The competition between the nonequilibrium effect and the larger distance effect lead to the up and down behavior of the quantum correlation with respect to the acceleration difference. We notice that eventually as the acceleration difference becomes larger, the nonequilibrium effects dominate over the distance effect. The quantum correlations reach the maximum as the acceleration difference becomes very large within the cavity range.



(8a)



(8b)



(8c)

Figure (8a) describes how  $E_N$  varies with respect to the acceleration difference and time. Alice stays at a lower acceleration  $0.02\pi$  and Bob has a larger acceleration starting from  $\pi$ . Figure (8b) describes how mutual information varies with respect to the acceleration difference and time. Alice stays a lower acceleration  $0.02\pi$ , and Bob has a larger acceleration starting from  $\pi$ . Figure (4c) describes how quantum discord varies with respect to the acceleration difference and time. Alice stays at lower acceleration  $0.02\pi$  and Bob has a larger acceleration starting from  $\pi$ . All the parameters are the same as those in Figure (1a) (1b).

#### IV. Conclusion

Using the developed methods, we discuss the difference of the equilibrium quantum correlations such as entanglement, mutual information and quantum discord between the two equally accelerated detectors and that between the two stationary detectors in thermal field with temperature  $T$ . They behave somewhat alike at less acceleration (or temperature). There are several ups and downs over time. However, at larger acceleration, their behaviors are quite different, which is partly due to the redshift of the accelerated detectors. As the temperature of the stationary detectors increase, the entanglement will disappear, while the mutual information and the quantum discord can be enlarged. The reason has been studied: the quantum discord (mutual information) is sustained due to the dominant system-environment (detector-field) entanglement over the decoherence or the disentanglement from the system (detector-detector). On the other hand, the system-environment entanglement does not boost the entanglement within or between the systems. Indeed, due to monogamy, the entanglement is usually further damaged. However, in the accelerated case, as the acceleration of the detectors increases, the entanglement, mutual information and quantum discord will first increase and eventually decay. We suggest this is mainly the result from redshift. The quantum correlation between the detectors accelerated in the opposite direction has also been studied. It is shown that as the distance increases, the correlation will decay. Remarkably, the entanglement seems to be more robust than the other two correlations in this case.

In the meanwhile, we also study the nonequilibrium quantum correlations. We first consider the nonequilibrium effect caused by different couplings. We pointed out that the nonequilibriumness characterized by the degree of the detailed balance breaking caused by different couplings can increase the quantum correlation. Another nonequilibrium case we

consider is that the two accelerated detectors with different accelerations. This generates both the nonequilibrium effect and the distance effect on the quantum correlations between the two detectors. The nature of the nonequilibriumness is from the net energy flow to the system. Since the mass and energy is equivalent under the Einstein mass-energy relationship, the increase of the nonequilibriumness leads to the increase of the energy flow and therefore the effective mass of the system. Since the local curvature of the space-time geometry is dependent on the mass of the system, the increase of the nonequilibriumness can enhance the effective space-time curvature. An increased curvature can create space time fluctuations or short cut. This decreases significantly the effective distance for the communications. Thus one expects the nonequilibriumness can boost the quantum correlations through enhancing the effective curvature of the space-time geometry or generating the space-time short cut.

## Appendix

For a general time-dependent, quadratic Hamiltonian, it's convenient to express as the form of annihilation (creation) operator vector, which is defined as follow

$$\hat{\mathbf{a}} := [\hat{a}_{d_1}, \hat{a}_{d_2}, \hat{a}_{d_3} \cdots \hat{a}_{d_j}, \hat{a}_1, \hat{a}_2, \hat{a}_3 \cdots \hat{a}_N]^T \quad (\text{a.1})$$

$$\hat{\mathbf{a}}^\dagger := [\hat{a}_{d_1}^\dagger, \hat{a}_{d_2}^\dagger, \hat{a}_{d_3}^\dagger \cdots \hat{a}_{d_j}^\dagger, \hat{a}_1^\dagger, \hat{a}_2^\dagger, \hat{a}_3^\dagger \cdots \hat{a}_N^\dagger]^T \quad (\text{a.2})$$

A general quadratic Hamiltonian like (11) can be written as

$$\hat{\mathbf{H}}^H(t) = (\hat{\mathbf{a}}^\dagger)^T \mathbf{w}(t) \hat{\mathbf{a}} + (\hat{\mathbf{a}}^\dagger)^T \mathbf{m}(t) \hat{\mathbf{a}}^\dagger + \hat{\mathbf{a}}^T \mathbf{m}(t)^H \hat{\mathbf{a}} \quad (\text{a.3})$$

where  $\mathbf{w}(t)$  and  $\mathbf{m}(t)$  are coefficient matrices, and  $\mathbf{m}(t)^H$  is conjugate transpose of  $\mathbf{m}(t)$ ,  $\mathbf{m}(t)^H = \mathbf{m}(t)^{T*}$ . Combine (15) and (a.3), one obtains the matrix form of  $\mathbf{F}(t)$  as follow

$$\mathbf{F}(t) = \begin{pmatrix} \mathbf{A}(t) & \mathbf{C}(t) \\ \mathbf{C}(t)^H & \mathbf{B}(t) \end{pmatrix} \quad (\text{a.4})$$

where

$$\mathbf{A}(t) = \frac{1}{2}(\mathbf{w}(t) + \mathbf{m}(t) + \mathbf{m}(t)^H) \quad (\text{a.5})$$

$$\mathbf{B}(t) = \frac{1}{2}(\mathbf{w}(t) - \mathbf{m}(t) - \mathbf{m}(t)^H) \quad (\text{a.6})$$

$$\mathbf{C}(t) = \frac{1}{2}(\mathbf{w}(t) - \mathbf{m}(t) + \mathbf{m}(t)^H) \quad (\text{a.7})$$

## Reference

- [1]Nielsen, Michael a, Chuang, Isaac L. Quantum Computation and Quantum Information: 10th Anniversary Edition[M]. Cambridge University Press, 2011.
- [2]Einstein A , Podolsky B , Rosen N . Phys. Rev. 47, 777 (1935): Can Quantum-Mechanical Description of Physical Reality Be Considered Complete?[J]. 1935, 47(10):777-780.
- [3]Horodecki R , Horodecki P , Horodecki M , et al. Quantum entanglement[J]. Review of Modern Physics, 2007.
- [4]Belavkin V P , Ohya M . Entanglement, Quantum Entropy and Mutual Information[J]. Proceedings Mathematical Physical & Engineering ences, 2002, 458(2017):209-231.
- [5] H. Ollivier and W. H. Zurek, Phys. Rev. Lett. 88, 017901 (2001)
- [6]Adesso G , Fuentes-Schuller I , Ericsson M . Continuous variable entanglement sharing in non-inertial frames[J]. Physical Review A, 2007.
- [7]Fuentes-Schuller I , Mann R B . Alice falls into a black hole: Entanglement in non[J]. physical review letters, 2004.
- [8]Alsing P M , Fuentes-Schuller I , Mann R B , et al. Entanglement of Dirac fields in non-inertial frames[J]. Physical Review A, 2006, 74(3):396-401.
- [9]Ball J L , Fuentes-Schuller I , Schuller F P . Entanglement in an expanding spacetime[J]. 2006, 359(6):550-554.
- [10]Ling Y , He S , Qiu W , et al. Quantum entanglement of electromagnetic field in non-inertial reference frames[J]. Journal of Physics A Mathematical & Theoretical, 2007, 65(30):9025-9032.
- [11]Mart ́n-Mart ́nez, Eduardo, Menicucci N C . Cosmological quantum entanglement[J]. Classical & Quantum Gravity, 2012, 29(22):224003.
- [12]Mart ́n-Mart ́nez, Eduardo, Menicucci N C . Entanglement in curved spacetimes and cosmology[J]. Classical & Quantum Gravity, 2014, 31(21).
- [13]Unruh, W. G . Notes on black-hole evaporation[J]. Physical Review D Particles & Fields, 1976, 14(4):870-892.
- [14]Hawking S W . Particle Creation by Black Holes[M]// Hawking on the Big Bang and Black Holes. 1993.
- [15]Anthony Zee and Gino Segrè Quantum Field Theory in a Nutshell (second edition)[J]. American Journal of Physics, 2010, 78(9).
- [16]B. DeWitt, General Relativity; an Einstein Centenary Survey (Cambridge University Press, Cambridge, UK, 1980).
- [17]Crispino L C B , Higuchi A , Matsas G E A . The Unruh effect and its applications[J]. Reviews of Modern Physics, 2007, 80(3):787-838.
- [18]Mart ́n-Mart ́nez, Eduardo, Brown E G , Donnelly W , et al. Sustainable entanglement production from a quantum field[J]. Physical Review A, 2013, 88(5):11592-11604.
- [19]Allison Sachs, Robert B. Mann, Eduardo Mart ́n-Mart ́nez. Entanglement harvesting and divergences in quadratic Unruh-DeWitt detector pairs[J]. Physical Review D, 2017.
- [20]Lin S Y , Chou C H , Hu B L . Disentanglement of two harmonic oscillators in relativistic motion[J]. Physical Review D, 2008, 78(12):667-670.
- [21]Lin S Y , Hu B L . Entanglement creation between two causally-disconnected objects[J].

- Physical Review D Particles & Fields, 2009, 81(4):389-398.
- [22] Brown E G, Martín-Martínez E, Menicucci N C, et al. Detectors for probing relativistic quantum physics beyond perturbation theory[J]. Physical Review D, 2013, 87(8): 084062.
- [23] Brown, Eric G . Thermal amplification of field-correlation harvesting[J]. Physical Review A, 2013, 88(6):062336.
- [24] Adesso G , Ragy S , Lee A R . Continuous variable quantum information: Gaussian states and beyond[J]. Open Systems & Information Dynamics, 2014, 21(01n02):1440001-.
- [25] Adesso G , Illuminati F . Entanglement in continuous variable systems: Recent advances and current perspectives[J]. Journal of Physics A General Physics, 2007, 40(28):7821-7880.
- [26] Adesso G, Datta A. Quantum versus classical correlations in Gaussian states[J]. Physical review letters, 2010, 105(3): 030501.
- [27] Bellomo B , Franco R L , Compagno G . Non-Markovian effects on the dynamics of entanglement[J]. Physical Review Letters, 2007, 99(16):160502.
- [28] Fanchini F F , Cornelio M F , De Oliveira M C , et al. Conservation law for distributed entanglement of formation and quantum discord[J]. Physical Review A, 2010, 84(1):012313.
- [29] Madhok V , Gupta V , Trottier D A , et al. Signatures of chaos in the dynamics of quantum discord[J]. Physical Review E, 2015, 91(3):032906.